SIAM J. Appl. Math.
Vol. 84, No. 4, pp. 1557–1579

JOINT IMPACT OF MATURATION DELAY AND FEAR EFFECT ON THE POPULATION DYNAMICS OF A PREDATOR-PREY SYSTEM*

XIAOKE MA†, YING SU†, AND XINGFU ZOU‡

Abstract. In this paper, taking into account the maturation period of prey, we propose a predator-prey model with time delay and fear effect. We confirm the well-posedness of the model system, explore the stability of the equilibria and uniform persistence of the model, and investigate Hopf bifurcations. Moreover, we also numerically explore the global continuation of the Hopf bifurcation. Interestingly, our results show that as the delay increases, the stable and unstable periodic solutions may both disappear and the unstable positive equilibrium may regain its stability. These results reveal how the maturation delay and the fear effect jointly impact the population dynamics of the predator-prey system.

Key words. predator-prey system, fear effect, maturation delay, stability, Hopf bifurcation, bistability

MSC codes. 34K13, 34K20, 37N25, 92B05

DOI. 10.1137/23M1596569

1. Introduction.

The study of interactions between prey and predators has always been a hot topic in ecology and evolutionary biology. Since Lotka [23] and Volterra [36] developed the well-known predator-prey model, a large body of literature has been devoted to the study of the mechanisms that drive the predator-prey system. A generalized ODE predator-prey model can be described as follows:

$$\begin{cases} \dfrac{\mathrm{d}u}{\mathrm{d}t} = p_1(u) - g(u,v)v, \\ \dfrac{\mathrm{d}v}{\mathrm{d}t} = p_2(v) + cg(u,v)v, \end{cases}$$

where $u(t)$ and $v(t)$ represent, respectively, the populations of prey and predator at time t, $p_1(u)$ is the growth rate of prey in the absence of a predator, $p_2(u)$ is the growth rate of predator in the absence of prey, $g(u,v)$ is the functional response reflecting the predation rate and biomass transfer, and c is the conversion efficiency of biomass from prey to predator. Following the classic Lotka–Volterra model, more and more functional response functions have been proposed, and the resulting ODE models have been widely studied. These include Holling types of responses [18], nonmonotone functional response [29], Beddington–DeAngelis functional response [4, 10], ratio-dependent functional response [33], and so on.

However, most of existing studies focus on understanding the direct influence of predators on prey. In other words, predators only affect the prey by directly killing and consuming them. In reality, most of the prey show a variety of antipredation

---

[*] Received by the editors August 28, 2023; accepted for publication (in revised form) May 2, 2024; published electronically July 22, 2024.
https://doi.org/10.1137/23M1596569
Funding: This work was partially supported by the NSF of China (11971129) and NSERC of Canada (RGPIN-2022-04744).

[†] School of Mathematics, Harbin Institute of Technology, Harbin, 150001, People's Republic of China (821530557@qq.com, ysu@hit.edu.cn).
[‡] Corresponding author. Department of Mathematics, University of Western Ontario, London, ON N6A 5B7, Canada (xzou@uwo.ca).

behaviors when they perceive predation risk, including changes in foraging behaviors [1] and vigilance and physiological changes [7, 6]. Such antipredation behaviors will bring a cost to the prey population [14]. In 2011, Zanette et al. [41] found, in a field experiment on song sparrow population, that the fear of the predator on the birds could lead to as large as a 40% reduction in song sparrow offspring.

The above biological studies suggest that it is unreasonable to ignore the indirect effect due to fear in the classical predator-prey model. To explain the fear effect mathematically, in 2016, Wang, Zanette, and Zou [37] first proposed the following predator-prey model:

$$\begin{cases} \dfrac{\mathrm{d}u}{\mathrm{d}t} = f(k,v)r_0u - du - au^2 - g(u)v, \\ \dfrac{\mathrm{d}v}{\mathrm{d}t} = cg(u)v - mv, \end{cases} \tag{1.1}$$

where r_0 is the natural birth rate of prey in the absence of predators, k reflects the fear level of the prey due to perceiving the risk of predation, $f(k,v)$ is the cost of the antipredation defense of the prey due to fear and it is monotonically decreasing in k and v, d is the natural death rate of prey, a is the density-dependent death rate of the prey due to intraspecies competition, $g(u)$ is the functional response function which is independent of v, and m is the predator death rate. Through mathematical analysis and numerical simulations, the authors of [37] obtained some interesting results on how the fear effect affects the dynamical behaviors of the predator-prey model. Since [37], there have occurred a large number of publications on modeling various aspects of the fear effect in predator-prey interactions by a variety of types of differential equations models, including ordinary differential equations [15, 24, 20, 42, 3, 25], reaction-diffusion equations [35, 39, 22], stochastic dynamical models [9, 27], functional differential equations [38, 19, 26, 40, 12], and partial functional differential equations [11, 8]. In addition, other types of models, including the discrete time model [2] and discrete space model [21], have also been proposed.

Among the aforementioned functional (or delay) differential equation models with fear effect, Wang and Zou [38] proposed and analyzed the following model incorporated with age structure and level of antipredator defense of adult prey:

$$\begin{cases} \dfrac{\mathrm{d}u_1}{\mathrm{d}t} = b(k,u_2)u_2 - (d_0+d_1k)u_1 - (s_0+s_1k)u_1v \\ \qquad\qquad -b(k,u_2(t-\tau))u_2(t-\tau)e^{-(d_0+s_0v+(d_1+s_1v)k)\tau}, \\ \dfrac{\mathrm{d}u_2}{\mathrm{d}t} = b(k,u_2(t-\tau))u_2(t-\tau)e^{-(d_0+s_0v+(d_1+s_1v)k)\tau} - d_2u_2 - s(k)u_2v, \end{cases} \tag{1.2}$$

where u_1 and u_2, respectively, represent the population density of juvenile prey and adult prey, τ is maturation delay, and the population density of predators v *is assumed to be a constant.* The assumption of a constant predator population reduces the number of equations and greatly simplifies the analysis of (1.2). For example, when the antipredation response level k is also a constant, then the second equation in (1.2) actually decouples from the first equation, and thus, as pointed out in (1.2), the population dynamics of the prey are determined by a scalar delay differential equation (DDE) of the form

$$u'(t) = e^{-\delta\tau}f(u(t-\tau)) - du(t),$$

which has been widely studied for various nonlinearities of $f(u)$. However, in many predator-prey interactions, it is not realistic to assume a constant predator population, and dropping such an assumption may lead to different population dynamics in the predator-prey system. Even if assuming a constant predator population, when the response level k also evolves according to some rules, the analysis of (1.2) is still very challenging, and hence only some preliminary results are obtained and the dynamics of (1.2) remain largely open.

For other delay models mentioned above, in Panday et al. [26], a delay representing the time lag between the perception of predation risk and the occurrence of antipredation behaviors—fear response delay, for short—was considered, and the authors show that the large value of delay has a destabilizing effect and can cause chaos. In Kumar and Dubey [19] and Wang and Zou [40], a gestation delay was incorporated in the respective models to account for the time needed for the biomass to be transferred from the prey to the predator after predation, where the gestation delay is also found to play a destabilizing role. In Dubey, Sanjan, and Kumar [12], in addition to the gestation delay, fear response delay was also introduced, just as in Panday et al. [26]. The authors investigated how the fear effect and the two delays impact the dynamics of the predator-prey system, and they also found that large delay will cause the coexistence equilibrium to lose its stability.

Dropping the assumption of constant predator population as in (1.1) and considering the maturation delay as in (1.2) lead to the following new predator-prey system:

$$\begin{cases} \dfrac{\mathrm{d}u(t)}{dt} = e^{-d_0\tau} f(k, v(t-\tau)) r_0 u(t-\tau) - du(t) - au^2(t) - g(u(t))v(t), \\ \dfrac{\mathrm{d}v(t)}{dt} = cg(u(t))v(t) - mv(t). \end{cases} \tag{1.3}$$

Here $u(t)$ is the population of *adult prey* and $v(t)$ is the population of the predator, $g(u)$ is the functional response, and c reflects the efficiency of biomass transfer from prey to predator. The constants d and a represent the density-independent and density-dependent death rates of adult prey, respectively; τ is the maturation duration of the prey and d_0 is the death rate of immature prey and, accordingly, $e^{-d_0\tau}$ represents the survival rate of prey from juvenile to adult. The constant r_0 is the birth rate of the prey, and the function $f(k,v)$, with k being the antipredation response level as in (1.1), accounts for the cost of the response in production. By the biological meanings of k and $f(k,v)$, the following conditions on $f(k,v)$ are imposed:

$$f(k,0) = f(0,v) = 1,\ \frac{\partial f}{\partial k} \le 0,\ \frac{\partial f}{\partial v} \le 0,\ \lim_{k\to+\infty} f(k,v) = \lim_{v\to+\infty} f(k,v) = 0.$$

To be more specific, we adopt $f(k,v) = 1/(1+kv)$ and choose $g(u)$ be a Holling Type II functional response function, leading to the following DDE model system:

$$\begin{cases} \dfrac{\mathrm{d}u(t)}{dt} = e^{-d_0\tau} \dfrac{r_0 u(t-\tau)}{1+kv(t-\tau)} - du(t) - au^2(t) - \dfrac{pu(t)v(t)}{1+qu(t)}, \\ \dfrac{\mathrm{d}v(t)}{dt} = c\dfrac{pu(t)v(t)}{1+qu(t)} - mv(t), \end{cases} \tag{1.4}$$

where p is the consuming rate of the predator per unit time, and q is the fixed handling time for a predator to capture each prey. Note that this is a nonmonotone DDE system, and the nonmonotonicity comes from two sources: (i) the nature of predator-prey interaction, and (ii) the negative delayed feedback reflected by the term $v(t-\tau)$.

The goal of this paper is to analyze the new DDE model system (1.4). The rest of this paper is organized as follows. In section 2, the well-posedness of the system

(1.4) with the biological initial conditions is established, including the existence and uniqueness, the positivity, and the eventually uniform boundedness. In section 3, we investigate the existence and stability of equilibria, the uniform persistence of the solution, and the existence of Hopf bifurcation. In section 4, we obtain the properties of Hopf bifurcation and the bifurcated periodic solutions which demonstrate different bifurcation paths with respect to the delay parameter from those in [12, 19, 26, 40]. In section 5, we provide some numerical simulations to investigate the influence of delay and demonstrate our mathematical results. In section 6, we briefly summarize our work and explain its biological implications.

2. Well-posedness of model (1.4).

Considering the population background, the following nonnegative initial functions should be associated with (1.4):

$$(u(\theta), v(\theta)) = (u_0(\theta), v_0(\theta)) \in \mathcal{C}\left([-\tau, 0], \mathbb{R}^2_+\right) =: \mathcal{C}_+. \tag{2.1}$$

We first confirm the well-posedness of (1.4)–(2.1), as stated in the following theorem.

Theorem 2.1. *For any* $(u_0, v_0)^T \in \mathcal{C}_+$, *system* (1.4) *has a unique solution satisfying* (2.1), *which exists globally in* $(0, +\infty)$, *is nonnegative, and remains bounded. Moreover, the region*

$$\Omega := \left\{(u,v) \in \mathcal{C}_+ : 0 \leqslant u \leqslant (r_0 e^{-d_0\tau} - d)/a,\ 0 \leqslant v/c + u < L_0\right\}$$

is both positively invariant and attractive for (1.4), *where*

$$L_0 := \frac{r_0 e^{-d_0\tau}(r_0 e^{-d_0\tau} - d)}{\delta a}.$$

Proof. For any $(u_0, v_0)^T \in \mathcal{C}_+$, by the fundamental theory of functional differential equations, system (1.4) has a unique solution $(u(t, u_0, v_0), v(t, u_0, v_0))^T$ on a maximal interval $[0, \sigma)$. From [32, Theorem 5.2.1], it is easy to see that the solution remains nonnegative for all $t \in [0, \sigma)$. To show the solution is bounded, we first note that

$$u'(t) \leqslant r_0 e^{-d_0\tau} u(t-\tau) - du(t) - au^2(t) \leqslant r_0 e^{-d_0\tau} u(t-\tau) - du(t). \tag{2.2}$$

This means that the first equation in (1.4) has an upper comparing equation

$$w'(t) = r_0 e^{-d_0\tau} w(t-\tau) - dw(t) \tag{2.3}$$

which is a linear DDE that satisfies the quasi-monotone condition (hence monotone). If $r_0 e^{-d_0\tau} - d < 0$, then every solution of (2.3) converges to zero, while when $r_0 e^{-d_0\tau} - d > 0$, every solution of (2.3) converges to $(r_0 e^{-d_0\tau} - d)/a$. By the comparison theorem for functional differential equations [32], we have

$$\limsup_{t \to +\infty} u(t) \leqslant \frac{r_0 e^{-d_0\tau} - d}{a}. \tag{2.4}$$

Thus, for any $\varepsilon > 0$, there exists $t_0 > 0$ such that $u(t) \leqslant (r_0 e^{-d_0\tau} - d)/a + \varepsilon$ for $t > t_0$. Let $L(t) = u(t) + v(t)/c$. By direct calculations, we have

$$\begin{aligned}\frac{\mathrm{d}L(t)}{\mathrm{d}t} &= \frac{r_0 e^{-d_0\tau} u(t-\tau)}{1 + kv(t-\tau)} - du(t) - au^2(t) - \frac{m}{c} v(t)\\ &\leqslant r_0 e^{-d_0\tau} u(t-\tau) - \delta L(t),\end{aligned}$$

where $\delta = \min\{d,\, m/c\}$. When $t > t_0 + \tau$, $u(t-\tau) \leqslant (r_0 e^{-d_0\tau} - d)/a + \varepsilon$, which leads to

$$\frac{\mathrm{d}L(t)}{\mathrm{d}t} \leqslant r_0 e^{-d_0\tau}\left[\frac{r_0 e^{-d_0\tau} - d}{a} + \varepsilon\right] - \delta L(t), \ \ t \geq t_0 + \tau.$$

This implies

$$\limsup_{t\to+\infty} L(t) \leqslant \frac{r_0 e^{-d_0\tau}}{\delta}\left[\frac{r_0 e^{-d_0\tau} - d}{a} + \varepsilon\right].$$

Since $\varepsilon > 0$ is arbitrary, letting $\varepsilon \to 0$ leads to

$$\limsup_{t\to+\infty} L(t) \leqslant \frac{r_0 e^{-d_0\tau}(r_0 e^{-d_0\tau} - d)}{\delta a} = L_0. \tag{2.5}$$

The estimates of (2.4) and (2.5) confirm the boundedness of the solution, implying that $\sigma = \infty$. The two estimates, together with the nonnegativity of the solution, also show that Ω is indeed positively invariant and attractive, completing the proof. ☐

3. Equilibria and their stability analysis.

In this section, we study the long-time dynamical behaviors of solutions of system (1.4)–(2.1) by analyzing existence and stability of equilibria and the existence of Hopf bifurcation.

3.1. Existence and stability of boundary equilibria.

Obviously, system (1.4) always has the trivial equilibrium $E_0 = (0,\, 0)$. In addition, the semitrivial equilibrium $E_1 = \big((r_0 e^{-d_0\tau} - d)/a, 0\big) =: (\hat{u}, 0)$ exists if $r_0 e^{-d_0\tau} > d$. The local stability/instability of E_0 and E_1 are given in the following theorem.

Theorem 3.1. *The following statements hold:*

- (i) *The trivial equilibrium E_0 is locally asymptotically stable if $r_0 e^{-d_0\tau} < d$ and is unstable if $r_0 e^{-d_0\tau} > d$.*
- (ii) *The boundary equilibrium E_1 exists if $r_0 e^{-d_0\tau} > d$. When E_1 exists, it is locally asymptotically stable if*

$$(r_0 e^{-d_0\tau} - d)(cp - mq) < am \tag{3.1}$$

and is unstable if

$$(r_0 e^{-d_0\tau} - d)(cp - mq) > am. \tag{3.2}$$

Proof. (i) The characteristic equation of (1.4) at E_0 is

$$\left(\lambda + d - r_0 e^{-d_0\tau} e^{-\lambda\tau}\right)(\lambda + m) = 0.$$

Observe that $\lambda = -m < 0$ is a negative root and other roots are determined by the equation $\lambda + d - r_0 e^{-d_0\tau} e^{-\lambda\tau} = 0$. By [30, Theorem 4.7], if $r_0 e^{-d_0\tau} - d < 0$, E_0 is locally asymptotically stable; if $r_0 e^{-d_0\tau} - d > 0$, E_0 is unstable.

(ii) Assume $r_0 e^{-d_0\tau} > d$ so that E_1 exists. The characteristic equation of (1.4) at E_1 is

$$\left(\lambda - d + 2r_0 e^{-d_0\tau} - r_0 e^{-d_0\tau} e^{-\lambda\tau}\right)\left(\lambda - \frac{cp\hat{u}}{1 + q\hat{u}} + m\right) = 0.$$

Since $-d + 2r_0 e^{-d_0\tau} > 0 > -r_0 e^{-d_0\tau}$ and $r_0 e^{-d_0\tau} > d$, all roots of the equation

$$\lambda - d + 2r_0 e^{-d_0\tau} - r_0 e^{-d_0\tau} e^{-\lambda\tau} = 0$$

have strictly negative real parts (see, e.g., [30, Theorem 4.7]). Thus, if condition (3.1) holds, $\lambda = cp\hat{u}/(1+q\hat{u}) - m < 0$, which means that E_1 is locally asymptotically stable, and if condition (3.2) holds, E_1 is unstable. ∎

Indeed, by a properly chosen Lyapunov function for E_0 and by a comparison argument for E_1, we can address the global asymptotic stability of E_0 and E_1, as is done in the next two theorems.

Theorem 3.2. *If $r_0 e^{-d_0\tau} \leqslant d$ holds, E_0 is globally asymptotically stable.*

Proof. If $r_0 e^{-d_0\tau} < d$, let $V(t)$ be defined by

$$V(t) = u(t) + \frac{v(t)}{c} + r_0 e^{-d_0\tau} \int_{t-\tau}^{t} \frac{u(s)}{1+kv(s)} \mathrm{d}s.$$

Taking the derivative of $V(t)$ along the trajectory of (1.4) yields

$$V'(t) = -\left[d - \frac{r_0 e^{-d_0\tau}}{1+kv(t)}\right] u(t) - au^2(t) - \frac{m}{c} v(t) \leq 0,$$

and $V'(t) = 0$ if and only if $u(t) = v(t) = 0$. By the LaSalle Invariance Principle (see, e.g., [16]), $u(t) \to 0$, $v(t) \to 0$ as $t \to \infty$, implying the global asymptotic stability of E_0. ∎

Theorem 3.3. *Assume $r_0 e^{-d_0\tau} > d$ so that E_1 exists. If condition* (3.1) *holds, then E_1 is globally asymptotically stable.*

Proof. Note that $u'(t) \leqslant r_0 e^{-d_0\tau} u(t-\tau) - du(t) - au^2(t)$. The right-hand side of the above inequality defines a monotone linear delay differential equation

$$x'(t) = r_0 e^{-d_0\tau} x(t-\tau) - dx(t) - ax^2(t), \tag{3.3}$$

which has the positive equilibrium $(r_0 e^{-d_0\tau}) - d)/a$ as a globally asymptotically stable equilibrium. By the comparison theorem for DDEs (see, e.g., [32]), we have

$$\limsup_{t\to\infty} u(t) \leqslant \frac{r_0 e^{-d_0\tau} - d}{a}.$$

Thus, for any $\varepsilon > 0$ there is a $T(\varepsilon) > 0$ such that $u(t) < \hat{u} + \varepsilon$ for any $t > T(\varepsilon)$. Then, for $t > T(\varepsilon)$, the ODE for $v(t)$ satisfies

$$v'(t) \leqslant \frac{cp\,(\hat{u}+\varepsilon)\,v(t)}{(1+k_2 v(t))\,[1+q\,(\hat{u}+\varepsilon)]} - mv \leqslant \left[\frac{cp\,(\hat{u}+\varepsilon)}{1+q\,(\hat{u}+\varepsilon)} - m\right] v(t),$$

Since condition (3.1) holds, we can choose ε small enough such that $\frac{cp(\hat{u}+\varepsilon)}{1+q(\hat{u}+\varepsilon)} < m$, which implies, again by the comparison principle of ODE (see, e.g., [32]), that $v(t) \to 0$ as $t \to \infty$. This means that the first equation in (1.4) has (3.3) as its limit equation. By the theory of asymptotically autonomous systems [34], we conclude that $u(t) \to \frac{r_0 e^{-d_0\tau} - d}{a}$ as $t \to \infty$. The proof is complete. ∎

Next, we discuss what happens when E_1 exists but is not stable, that is, when $r_0 e^{-d_0\tau} > d$ but (3.1) is reversed (i.e., (3.2) holds).

Theorem 3.4. *System* (1.4) *is uniformly persistent when $r_0 e^{-d_0\tau} > d$ and condition* (3.2) *holds, in the sense that there exists $\eta > 0$ such that for every positive solution $(u(t), v(t))$, there hold*

$$\liminf_{t\to\infty} u(t) \geq \eta \quad \textit{and} \quad \liminf_{t\to\infty} v(t) \geq \eta.$$

Proof. For any $\phi \in \mathcal{C}_+$, let $X(t,\phi) = (u(t,\phi), v(t,\phi))^T$ be the solution satisfying this initial condition. Denote $\Phi(t)\phi = X_t(\phi)$ as the solution semiflow defined on $\mathcal{C}_+$. For our purpose of persistence, we consider the following distance function in $\mathcal{C}_+$:

$$p(\phi) = \min\{\phi_1(0), \phi_2(0)\}\ \forall \phi = (\phi_1, \phi_2) \in \mathcal{C}_+.$$

Denote the interior of the positive cone $\mathcal{C}_+$ by

$$X_0 := int\mathcal{C}_+ = \{\phi \in \mathcal{C}_+ : \phi(\theta) > 0, \theta \in [-\tau, 0]\},$$

which has the boundary $\partial X_0 = \mathcal{C}_+ \backslash X_0$ satisfying $X_0 \cap \partial X_0 = \emptyset$. We know that X_0 and ∂X_0 are positive invariant, meaning that $\Phi(t) : X_0 \to X_0$ and $\Phi(t) : \partial X_0 \to \partial X_0$. By the proof of the eventually uniform boundedness of the solution of system (1.4) in section 2, the bounded set Ω is a global attractor of Φ.

Note that system (1.4) has only two equilibria on ∂X_0, E_0 and E_1, which are both unstable. For any $\phi \in \partial X_0$, $\Phi(t)\phi \to E_0$ or E_1 as $t \to \infty$. Thus, the hypotheses $(C1)$ and $(C2)$ of [31, Theorem 3] are satisfied and the conclusion of that theorem holds, completing the proof. ☐

Comparing the above results with those for model (1.1), we have seen that the incorporation of the maturation delay τ can affect the stability of the trivial equilibrium E_0 as well as the existence and stability of the boundary equilibrium E_1. Indeed, expressing those conditions involved in Theorems 3.1–3.4, in terms of the delay τ, we can have the following theorem.

THEOREM 3.5. *The following statements hold:*

(i) *If* $r_0 \leqslant d$, E_0 *is globally asymptotically stable for any* $\tau \geqslant 0$.

(ii) *If* $r_0 > d$, *there exists a critical value*

$$\tau_* := \frac{1}{d_0} \ln \frac{r_0}{d} \tag{3.4}$$

such that E_0 *is globally asymptotically stable if* $\tau \geqslant \tau_*$ *but is unstable if* $\tau < \tau_*$.

(iii) *If* $r_0 > d$ *and* $\tau < \tau^*$, *then* E_1 *comes into existence; moreover,*

- (iii-a) *when* $(r_0 - d)(cp - mq) \leq am$ *(implying* (3.1) *holds),* E_1 *is globally asymptotically stable for all* $\tau \in (0, \tau^*)$;
- (iii-b) *when* $(r_0 - d)(cp - mq) > am$, *there exists a critical value*

$$\tau_{**} := \frac{1}{d_0} \ln \frac{r_0(cp - mq)}{am + d(cp - mq)} \tag{3.5}$$

such that E_1 *is globally asymptotically stable if* $\tau_{**} \leqslant \tau < \tau_*$ *(implying* (3.1) *holds);* E_1 *becomes unstable and* (1.4) *is persistent if* $\tau < \tau_{**}$ *(implying* (3.2) *holds).*

We point out that τ_* and τ_{**} are independent of k, and $\tau_{**} < \tau_*$. These obvious facts are useful in our further analysis in what follows, when we will use τ as the bifurcation parameter. In the next subsection, we will focus on the existence and the stability/instability of a positive equilibrium, as well as switches between the stability and instability through bifurcation analysis.

3.2. Existence and stability of the positive equilibrium and Hopf bifurcation.

In this subsection, we will focus on the scenario that E_1 exists but is unstable, that is, $r_0 e^{-d_0\tau} > d$ and (3.2) holds. The uniform persistence confirmed in

Theorem 3.4 together with abstract persistence theory implies the existence of a positive equilibrium for (1.4). However, in what follows, we will directly prove not only the existence but also uniqueness of a positive equilibrium under the above conditions.

Note that a positive equilibrium $E^* = (u^*,\ v^*)$ of (1.4) is a positive solution to the equations

$$\begin{cases} \dfrac{r_0 e^{-d_0\tau}}{1+kv} - d - au - \dfrac{pv}{1+qu} = 0, \\ \dfrac{cpu}{1+qu} = m. \end{cases}$$

It is easy to see that $u^* = \frac{m}{cp-mq}$, which is positive by (3.2), and v^* solves the following quadratic equation:

$$pkv^2 + [(d+au^*)(1+qu^*)k + p]\,v - (1+qu^*)(r_0 e^{-d_0\tau} - d - au^*) = 0.$$

Condition (3.2) guarantees that the constant term of the above quadratic equation is negative, which implies that the above quadratic equation has a unique positive root. This means that system (1.4) has a unique positive equilibrium E^*. Furthermore, u^* is independent of τ while $v^* = v^*(\tau)$ is decreasing in τ.

Note that model (1.4) with $\tau = 0$ becomes

$$\begin{cases} \dfrac{\mathrm{d}u}{\mathrm{d}t} = \dfrac{r_0 u}{1+kv} - du - au^2 - \dfrac{puv}{1+qu}, \\ \dfrac{\mathrm{d}v}{\mathrm{d}t} = \dfrac{cpuv}{1+qu} - mv. \end{cases} \tag{3.6}$$

For this ODE system, summarizing the results in [37], we have the following lemma on the stability of the positive equilibrium in terms of r_0 and k.

Lemma 3.6. *Assume $r_0 > d$ and condition (3.2) holds. Let*

$$r^* = \frac{am}{cp-mq} + d, \quad r^{**} = \frac{a(cp+mq)}{q(cp-mq)} + d,$$
$$k^* = \frac{q(cp-mq)^2((r_0-d)q(cp-mq) - a(cp+mq))}{c^2pa(qd(cp-mq) + a(cp+mq))}.$$

(i) *The positive equilibrium E^* of (3.6) is locally asymptotically stable, provided that*

$$r^* < r_0 \leqslant r^{**}, \tag{3.7}$$

or

$$r_0 > r^{**} \text{ and } k > k^*. \tag{3.8}$$

(ii) *Further assume that $k^* > 0$. If*

$$r_0 > r^{**} \text{ and } k < k^*, \tag{3.9}$$

then E^* is unstable.

(iii) *If $r_0 > r^{**}$ and $k^* > 0$, Hopf bifurcation occurs at $k = k^*$. Moreover, the bifurcations may be subcritical or supercritical.*

In order to investigate how the local stability of E^* changes with delay $\tau > 0$, we linearize system (1.4) at E^* to obtain

$$\begin{pmatrix} u'(t) \\ v'(t) \end{pmatrix} = \begin{pmatrix} J_{11} & J_{12} \\ J_{21} & 0 \end{pmatrix} \begin{pmatrix} u(t) \\ v(t) \end{pmatrix} + \begin{pmatrix} K_{11} & K_{12} \\ 0 & 0 \end{pmatrix} \begin{pmatrix} u(t-\tau) \\ v(t-\tau) \end{pmatrix}, \tag{3.10}$$

where

$$\begin{aligned} &J_{11} = -d - 2au^* - \tfrac{pv^*}{(1+qu^*)^2} < 0, \quad J_{12} = -\tfrac{m}{c} < 0, \\ &J_{21} = \tfrac{cpv^*}{(1+qu^*)^2} > 0, \quad K_{11} = \tfrac{r_0 e^{-d_0\tau}}{1+kv^*} > 0, \quad K_{12} = -\tfrac{kr_0 e^{-d_0\tau} u^*}{(1+kv^*)^2} < 0. \end{aligned} \tag{3.11}$$

Denote $P(\lambda,\tau) = \lambda^2 - J_{11}\lambda - J_{12}J_{21}$ and $Q(\lambda,\tau) = -K_{11}\lambda - J_{21}K_{12}$. Then the characteristic equation of the above linearized system is given by

$$P(\lambda,\tau) + e^{-\lambda\tau} Q(\lambda,\tau) = 0, \tag{3.12}$$

which is a quadratic exponential polynomial equation of λ with the coefficients depending on τ. We can use the geometric stability criterion for DDE with delay-dependent parameters developed in Beretta and Kuang [5]. To this end, we first give the following lemma.

Lemma 3.7. *$\lambda = 0$ is not the root of the characteristic equation (3.12) for all $\tau > 0$.*

Proof. Setting $\lambda = 0$, the characteristic equation becomes $-J_{21}(J_{12} + K_{12}) = 0$, which contradicts the sign of J_{21}, J_{12}, and K_{12}. The proof is complete. ☐

When $\tau = 0$, the distribution of characteristic roots of (3.12) is implied by Lemma 3.6. Particularly, when either (3.7) or (3.8) holds, all roots of (3.12) with $\tau = 0$ have negative real parts. Thus, when τ increases from $\tau = 0$, if (3.12) will ever have roots coming to the right half of the complex plane, such roots must be a result of a pair of complex roots crossing the pure imaginary axis from the left half to the right half on the complex plane for some positive value of τ. In what follows, we aim to find a pair of purely imaginary roots of (3.12) under condition (3.7) or (3.8). Note that (3.12) is an equation with τ-dependent parameters; we can employ the results in [5]. To this end, we first do some preparations below for the convenience of applying results in [5]:

(C1) By simplifying, we obtain

$$J_{11} + K_{11} = u^* \left(\frac{pqv^*}{(1+qu^*)^2} - a \right).$$

From Lemma 3.6, under either (3.7) or (3.8), we know that $(J_{11} + K_{11})|_{\tau=0} < 0$. As pointed out before, $v^*(\tau)$ is deceasing in τ. Thus, we indeed have $J_{11}+K_{11} < 0$ for all $\tau \in [0, \tau_{**})$, and accordingly, for any $\omega \in \mathbb{R}$ and $\tau \in [0, \tau_{**})$,

$$P(i\omega,\tau) + Q(i\omega,\tau) = -\omega^2 - J_{12}J_{21} - J_{21}K_{12} - i\omega(J_{11} + K_{11}) \neq 0.$$

Note that when (3.9) holds, by Lemma 3.6, there exist $\omega_0 > 0$ and $\tau_0 > 0$ such that $P(i\omega_0, \tau_0) + Q(i\omega_0, \tau_0) = 0$ and the above condition no longer holds.

(C2) Direct calculation shows that for all $\tau \in [0, \tau_{**})$, there holds

$$\begin{aligned} \limsup_{|\lambda|\to\infty} \left\{ \left| \frac{P(\lambda,\tau)}{Q(\lambda,\tau)} \right| : \mathrm{Re}\lambda \geqslant 0 \right\} &= \limsup_{|\lambda|\to\infty} \left\{ \left| \frac{-K_{11}\lambda - J_{21}K_{21}}{\lambda^2 - J_{11}\lambda - J_{21}J_{12}} \right| : \mathrm{Re}\lambda \geqslant 0 \right\} \\ &= 0 < 1. \end{aligned}$$

(C3) Direct calculations also give

$$|P(i\omega,\tau)|^2 = (\omega^2 + J_{12}J_{21})^2 + J_{11}^2\omega^2, \quad |Q(i\omega,\tau)|^2 = K_{11}^2\omega^2 + J_{21}^2K_{12}^2,$$

by which we obtain

$$\begin{aligned} F(\omega,\tau) &= |P(i\omega,\tau)|^2 - |Q(i\omega,\tau)|^2 \\ &= \omega^4 + (2J_{12}J_{21} + J_{11}^2 - K_{11}^2)\omega^2 + J_{21}^2(J_{12}^2 - K_{12}^2) \\ &=: \omega^4 + B(\tau)\omega^2 + C(\tau). \end{aligned} \tag{3.13}$$

(C4) By the implicit function theorem, as long as $F(\omega,\tau)=0$ has a positive root ω, this root $\omega=\omega(\tau)$ must be continuously differentiable with respect to τ.

Note that (3.13) is a quadratic function of ω^2 whose positive roots will contribute to the existence of Hopf bifurcation. More specifically, if $C(\tau) < 0$ holds for all $\tau \in [0,\tau_{**})$, $F(\omega,\tau)=0$ has a unique positive real root. Now, we analyze the existence of Hopf bifurcation on $[0,\tau_{**})$ by employing the theory of Beretta and Kuang in [5]. In what follows, we will confine ourselves to this case: $C(\tau)<0$.

Let $\lambda = \pm i\omega(\omega > 0)$ be the root of (3.12). Substituting it into (3.12) and separating the real and imaginary parts, we have

$$\begin{cases} J_{21}K_{12}\cos\omega\tau + K_{11}\omega\sin\omega\tau = -\omega^2 - J_{12}J_{21}, \\ K_{11}\omega\cos\omega\tau - J_{21}K_{12}\sin\omega\tau = -J_{11}\omega, \end{cases}$$

which leads to

$$\begin{cases} \cos\omega\tau = \frac{-(J_{21}K_{12}+J_{11}K_{11})\omega^2 - J_{21}^2J_{12}K_{12}}{K_{11}^2\omega^2+J_{21}^2K_{12}^2} =: P_0(\tau), \\ \sin\omega\tau = \frac{-K_{11}\omega^3+(J_{11}J_{21}K_{12}-K_{11}J_{21}J_{12})\omega}{K_{11}^2\omega^2+J_{21}^2K_{12}^2} =: Q_0(\tau). \end{cases} \tag{3.14}$$

On the other hand, if $\omega(\tau)$ satisfies (3.14), then $\omega(\tau)$ must satisfy $|P(i\omega,\tau)|^2 = |Q(i\omega,\tau)|^2$; that is, $\omega(\tau)$ must be a positive root of $F(\omega,\tau)=0$. If $F(\omega,\tau)=0$ has positive real root $\omega(\tau)$, then

$$\begin{cases} \cos\theta(\tau) = P_0(\tau), \\ \sin\theta(\tau) = Q_0(\tau) \end{cases}$$

will have solutions $\theta(\tau) \in [0,2\pi]$ satisfying $\omega(\tau)\tau = \theta(\tau) + 2n\pi$, $n = 0,1,2,\ldots$, which is equivalent to

$$S_n(\tau) = \tau - \frac{\theta(\tau)+2n\pi}{\omega(\tau)} = 0, \ \tau \in [0,\tau_{**}), \ n = 0,1,2,\ldots. \tag{3.15}$$

Indeed, from (3.14), $\theta(\tau)$ can also be given by

$$\theta(\tau) = \begin{cases} \arccos P_0(\tau) & \text{if } Q_0(\tau) > 0, \\ 2\pi - \arccos P_0 & \text{if } Q_0(\tau) < 0. \end{cases}$$

That is, if there is a $\hat{\tau} \in [0,\tau_{**})$ such that $S_n(\hat{\tau}) = 0$ for some n, then there exists a pair of simple conjugate pure imaginary roots $\lambda_{\pm}(\hat{\tau}) = \pm i\omega(\hat{\tau})$ for the characteristic equation (3.12). Note that $S_n(0) = -(\theta(0)+2n\pi)/\omega(0) < 0$ and for any $\tau \in [0,\tau_{**})$, $n \in \mathbb{N}_0$, $S_{n+1}(\tau) < S_n(\tau)$. Also for the sign of Q_0 which is defined in (3.14), we have the following lemma.

LEMMA 3.8. *If condition (3.7) or (3.8) holds, then* $Q_0(\tau) > 0$ *for all* $\tau > 0$. *If (3.9) holds, then there exists a unique* $\tau_c \in (0, \tau_{**})$ *such that*

$$Q_0(\tau) \begin{cases} < 0, & \tau \in (0, \tau_c), \\ = 0, & \tau = \tau_c, \\ > 0, & \tau \in (\tau_c, \tau_{**}). \end{cases}$$

Proof. Let $\Delta = B^2(\tau) - 4C(\tau) > 0$ (note that we have assumed that $C(\tau) < 0$). Since $\omega^2 = (-B + \sqrt{\Delta})/2$, we have

$$\text{sign} Q_0 = \text{sign}\left\{ J_{11}J_{21}K_{12} + \frac{K_{11}}{2}\left(J_{11}^2 - K_{11}^2\right) - \frac{K_{11}}{2}\sqrt{\Delta} \right\}.$$

From (3.11), $J_{11}J_{21}K_{12} > 0$ and $K_{11}\sqrt{\Delta}/2 > 0$ for all $\tau \in (0, \tau_{**})$.

When (3.7) or (3.8) holds, the fact that $J_{11} - K_{11} < 0$ together with (C1) implies $J_{11}^2 - K_{11}^2 > 0$. Denote

$$A_1 = J_{11}J_{21}K_{12} + \frac{K_{11}}{2}\left(J_{11}^2 - K_{11}^2\right), \;\; A_2 = \frac{K_{11}}{2}\sqrt{\Delta}.$$

Then $\text{sign} Q_0 = \text{sign}\{A_1 - A_2\}$. Calculations give

$$A_1^2 - A_2^2 = (J_{11}^2 - K_{11}^2)\left[J_{21}^2 K_{12}^2 + K_{11}J_{21}\left(J_{11}K_{12} - K_{11}J_{12}\right)\right] > 0,$$

implying that $Q_0(\tau) > 0$ for all $\tau > 0$.

When condition (3.9) is true, $(J_{11} + K_{11})|_{\tau=0} > 0$. Note that $J_{11} + K_{11}$ decreases in τ and $\lim_{\tau \to \tau_{**}-}(J_{11} + K_{11}) = -a < 0$. Thus, there exists a unique $\tau_c \in (0, \tau_{**})$ such that $J_{11} + K_{11} > 0$ if $\tau < \tau_c$ and $J_{11} + K_{11} < 0$ if $\tau > \tau_c$. Therefore, if $\tau < \tau_c$, $J_{11}^2 - K_{11}^2 = (J_{11} + K_{11})(J_{11} + K_{11}) < 0$. Denote

$$A_3 = J_{11}J_{21}K_{12}, \; A_4 = \frac{K_{11}}{2}\left(K_{11}^2 - J_{11}^2 + \sqrt{\Delta}\right).$$

Then $\text{sign} Q_0 = \text{sign}\{A_3 - A_4\}$. By calculations, we obtain

$$A_3^2 - A_4^2 = (J_{11}^2 - K_{11}^2)\left[J_{21}^2 K_{12}^2 - (J_{11}^2 - K_{11}^2) - 2J_{12}J_{21} + 2\sqrt{\Delta}\right] < 0.$$

Hence, $Q_0 < 0$ for all $\tau \in (0, \tau_c)$. If $\tau = \tau_c$, $J_{11} = K_{11}$ and $\Delta = 4J_{21}^2 K_{12}^2$. Evidently, $Q_0(\tau_c) = 0$. The proof of $Q(\tau) > 0$ for $\tau \in (\tau_c, \tau_{**})$ is similar to the case of (3.7) or (3.8). The proof is complete. ∎

Next, we verify the transversality condition at any critical value $\tau = \hat{\tau}$. Let $\lambda(\tau)$ be the eigenvalue of (3.12) satisfying $\lambda(\hat{\tau}) = i\omega(\hat{\tau}) = i\hat{\omega}$. Thus,

$$\begin{aligned} \delta(\hat{\tau}) &:= \text{sign}\left\{ \left.\frac{\mathrm{d}\,\text{Re}\lambda}{\mathrm{d}\tau}\right|_{\tau=\hat{\tau}} \right\} = \text{sign}\left\{F'_\omega(\omega(\hat{\tau}), \hat{\tau})\right\} \cdot \text{sign}\left\{ \left.\frac{\mathrm{d}\,\mathrm{S_n}(\tau)}{\mathrm{d}\tau}\right|_{\tau=\hat{\tau}} \right\} \\ &= \text{sign}\left\{2\omega(\hat{\tau}) \cdot \sqrt{\Delta}\right\} \cdot \text{sign}\left\{ \left.\frac{\mathrm{d}\,\mathrm{S_n}(\tau)}{\mathrm{d}\tau}\right|_{\tau=\hat{\tau}} \right\} = \text{sign}\left\{ \left.\frac{\mathrm{d}\,\mathrm{S_n}(\tau)}{\mathrm{d}\tau}\right|_{\tau=\hat{\tau}} \right\}. \end{aligned} \tag{3.16}$$

If $\delta(\hat{\tau}) \neq 0$, the transversality condition is satisfied and Hopf bifurcation occurs at $\tau = \hat{\tau}$.

Combining the above analyses and the results in [5], we have proved the following theorem on the stability of E^* and existence of Hopf bifurcation for system (1.4) in terms of τ.

THEOREM 3.9. *Assume that* (3.7) *or* (3.8) *holds. If* $S_0(\tau)=0$, $\tau\in[0,\tau_{**})$ *has two positive real roots, denoted by* τ_1 *and* τ_2*, respectively, with* $\tau_1<\tau_2$*. Then* $\delta(\tau_1)>0$ *and* $\delta(\tau_2)<0$*, meaning that when* τ *increases, Hopf bifurcation occurs at* $\tau=\tau_1$ *and* $\tau=\tau_2$*. Moreover, if* $S_n(\tau)=0$ *has no other zeros for all* $n\geqslant 1$*, then the positive equilibrium* E^* *is locally asymptotically stable when* $\tau\in[0,\tau_1)\cup(\tau_2,\tau_{**})$*; it is unstable when* $\tau\in(\tau_1,\tau_2)$*, yielding its stability to a periodic solution arising from Hopf bifurcation.*

Next, we consider the case when condition (3.9) holds. By Lemma 3.8 and the definition of $S_n(\tau)$, $S_n(\tau)$ has a jump discontinuity at τ_c, but the characteristic equation (3.12) has no pure imaginary root when $\tau=\tau_c$. Therefore, if $\tau\in(0,\tau_c)$ or $\tau\in(\tau_c,\tau_{**})$, the existence of the pure imaginary roots of the characteristic equation (3.12) is still equivalent to the existence of zeros of $S_n(\tau)$, and the transversality condition can still be confirmed by using (3.16). With these observations, and by Lemma 3.7 and the conclusion of Ruan and Wei in [28], we then obtain the following theorem for the case when (3.9) holds.

THEOREM 3.10. *Assume that* (3.9) *holds. If* $S_0(\tau)=0$ *for* $\tau\in[0,\tau_{**})$ *has only one positive real root, denoted by* τ_3*, and* $\delta(\tau_3)<0$*, then Hopf bifurcation occurs at* $\tau=\tau_3$*. Moreover, if* $S_n(\tau)=0$ *has no other zeros for all* $n\geqslant 1$*, the positive equilibrium* E^* *is unstable when* $\tau\in[0,\tau_3)$ *and is locally asymptotically stable when* $\tau\in(\tau_3,\tau_{**})$*.*

This theorem and Lemma 3.6(ii) show that a longer maturation delay of the prey may help the otherwise unstable coexistence equilibrium E^* regain its stability, restoring from sustained oscillation to dynamics of convergence to equilibrium. This is in contrast to the more common effect of delay: delay can destroy the stability of a stable equilibrium through Hopf bifurcation.

4. Properties of Hopf bifurcation.

Through the analyses in the preceding sections, we have known that Hopf bifurcation will occur under the appropriate conditions. In this section, we always assume that Hopf bifurcation occurs at a critical value $\hat{\tau}$ for the parameter τ and $\pm i\hat{\omega}$ are a pair of purely imaginary roots of the corresponding characteristic equation for the linearized system of (1.4) at E^*. We will explore the properties of Hopf bifurcation, including the direction and stability.

Let $\tau=\hat{\tau}+\mu$. Thus, Hopf bifurcation occurs at $\mu=0$. Considering the following transformation $x(t)=u(\tau t)-u^*$, $y(t)=v(\tau t)-v^*$, our model (1.4) becomes the following functional differential equation in $\mathcal{C}([-1,0],\mathbb{R}^2_+)$:

$$\frac{\mathrm{d}X}{\mathrm{d}t}=L_\mu(X_t)+G(\mu,X_t), \tag{4.1}$$

where $X(t)=(x(t),y(t))^T\in\mathbb{R}^2_+$, $X_t(\theta)=X(t+\theta),\theta\in[-1,0]$, $L_\mu:\mathcal{C}([-1,0],\mathbb{R}^2_+)\to\mathbb{R}$, $G:\mathbb{R}\times\mathcal{C}([-1,0],\mathbb{R}^2_+)\to\mathbb{R}$, and the definitions of L_μ and G are as follows:

$$L_\mu\phi=(\hat{\tau}+\mu)\left[B_1\phi(0)+C_1\phi(-1)\right],\ G(\mu,\phi)=\begin{pmatrix} G_1(\mu,\phi)\\ G_2(\mu,\phi)\end{pmatrix},$$

where $\phi=(\phi_1,\phi_2)^T\in\mathcal{C}([-1,0],\mathbb{R}^2_+)$, and

$$B_1=\begin{pmatrix} -d-2au^*-\frac{pv^*}{1+qu^*}+\frac{pqu^*v^*}{(1+qu^*)^2} & -\frac{m}{c}\\ \frac{cpv^*}{1+qu^*}-\frac{cpqu^*v^*}{(1+qu^*)^2} & 0\end{pmatrix}=:\begin{pmatrix} b_1 & b_2\\ b_3 & 0\end{pmatrix},$$

$$C_1=\begin{pmatrix} \frac{r_0e^{-d_0(\hat{\tau}+\mu)}}{1+kv^*} & \frac{-r_0e^{-d_0(\hat{\tau}+\mu)}ku^*}{(1+kv^*)^2}\\ 0 & 0\end{pmatrix}=:\begin{pmatrix} c_1 & c_2\\ 0 & 0\end{pmatrix},$$

$$\begin{aligned} G_1(\mu,\phi) &= (\hat{\tau}+\mu)\left[m_1\phi_1(-1)\phi_2(-1)+m_2\phi_2^2(-1)+m_3\phi_1(-1)\phi_2^2(-1)+m_4\phi_2^3(-1)\right.\\ &\qquad \left.+(n_1-a)\phi_1^2(0)+n_2\phi_1(0)\phi_2(0)+n_3\phi_1^3(0)+n_4\phi_1^2(0)\phi_2(0)+h.o.t.\right],\\ G_2(\mu,\phi) &= -c(\hat{\tau}+\mu)\left[n_1\phi_1^2(0)+n_2\phi_1(0)\phi_2(0)+n_3\phi_1^3(0)+n_4\phi_1^2(0)\phi_2(0)+h.o.t.\right], \end{aligned}$$

where

$$\begin{aligned} m_1 &= -\frac{r_0e^{-d_0(\hat{\tau}+\mu)}k}{(1+kv^*)^2}, m_2 = -\frac{ku^*m_1}{1+kv^*}, m_3 = -\frac{km_1}{1+kv^*}, m_4 = \frac{k^2u^*m_1}{(1+kv^*)^2},\\ n_1 &= \frac{pqv^*}{(1+qu^*)^3}, n_2 = -\frac{p}{(1+qu^*)^2}, n_3 = -\frac{pq^2v^*}{(1+qu^*)^4}, n_4 = \frac{pq}{(1+qu^*)^3}. \end{aligned}$$

By the Riesz representation theorem, there exists a bounded variation function $\eta(\theta,\mu)$ in $\theta\in[-1,0]$ such that for any $\phi\in\mathcal{C}([-1,0],\mathbb{R}_+^2)$,

$$L_\mu\phi = \int_{-1}^{0} \mathrm{d}_\theta\eta(\theta,\mu)\phi(\theta).$$

In fact, we can choose $\eta(\theta,\mu) = (\hat{\tau}+\mu)\left[B_1\delta(\theta)-C_1\delta(\theta+1)\right]$, where δ is Dirac-delta function.

For $\phi\in\mathcal{C}([-1,0],\mathbb{R}_+^2)$, define

$$A(\mu)\phi(\theta) = \begin{cases} \dfrac{\mathrm{d}\phi(\theta)}{\mathrm{d}\theta}, & -1\leqslant\theta<0,\\ \displaystyle\int_{-1}^{0}\mathrm{d}_{\mathrm{s}}\eta(\mathrm{s},\mu)\phi(s), & \theta=0, \end{cases} \qquad R(\mu)\phi(\theta) = \begin{cases} 0, & -1\leqslant\theta<0,\\ G(\mu,\phi), & \theta=0. \end{cases}$$

Then the original model (1.4) is equivalent to the following abstract ODE:

$$\dot{X}_t = A(\mu)X_t + R(\mu)X_t. \tag{4.2}$$

For $\psi\in\mathcal{C}^1([0,1],(\mathbb{C}^2)^*)$, the adjoint operator A^* of $A(\mu)$ is defined as

$$A^*\psi(s) = \begin{cases} -\dfrac{\mathrm{d}\psi(\mathrm{s})}{\mathrm{ds}}, & 0<s\leqslant 1,\\ \displaystyle\int_{-1}^{0}\mathrm{d}\eta^T(\xi,0)\psi(-\xi), & s=0, \end{cases}$$

and a bilinear form

$$\langle\psi,\phi\rangle = \overline{\psi}(0)\phi(0) - \int_{-1}^{0}\int_{\xi=0}^{\theta}\overline{\psi}(\xi-\theta)\mathrm{d}\eta(\theta)\phi(\xi)\mathrm{d}\xi,$$

where $\phi\in\mathcal{C}([-1,0],\mathbb{R}_+^2)$, $\eta(\theta)=\eta(\theta,0)$. It can be shown that $\langle\psi,A\phi\rangle = \langle A^*\psi,\phi\rangle$, $\langle\lambda\psi,\phi\rangle = \overline{\lambda}\langle\psi,\phi\rangle$.

Since $\pm i\hat{\omega}$ are the eigenvalues of the original system (1.4) at the positive equilibrium E^*, $\pm i\hat{\omega}\hat{\tau}$ are the eigenvalues of $A(0)$ and they are also the eigenvalues of A^*. By a direct calculation, the vectors

$$q(\theta) = (1,\gamma)^Te^{i\hat{\omega}\hat{\tau}\theta}, \theta\in[-1,0] \text{ and } q^*(s) = D(1,\gamma^*)e^{i\hat{\omega}\hat{\tau}s}, s\in[0,1],$$

are the eigenvectors of $A(0)$ and A^* corresponding to the eigenvalues $i\hat{\omega}\hat{\tau}$ and $-i\hat{\omega}\hat{\tau}$, respectively, satisfying $\langle q^*(s),q(\theta)\rangle = 1$ and $\langle q^*,\overline{q}\rangle = 0$, where

$$\gamma = \frac{b_3}{i\hat{\omega}},\ \gamma^* = \frac{-b_2-c_2e^{-i\hat{\omega}\hat{\tau}}}{i\hat{\omega}},\ \overline{D} = \frac{1}{1+\gamma\overline{\gamma^*}+\hat{\tau}e^{-i\hat{\omega}\hat{\tau}}(c_1+c_2\gamma)}.$$

Using the relevant theory of Hassard, Kazarinoff, and Wan [17], we aimed to obtain the properties of Hopf bifurcation. For the solution X_t of (4.1) at $\mu=0$, define

$$z(t)=\langle q^*, X_t\rangle \quad \text{and} \quad W(t,\theta)=X_t(\theta)-z(t)q(\theta)-\overline{z}(t)\overline{q}(\theta).$$

On the central manifold C_0, $W(t,\theta)=W(z,\overline{z},\theta)$, where

$$W(z,\overline{z},\theta)=W_{20}(\theta)\frac{z^2}{2}+W_{11}(\theta)z\overline{z}+W_{02}(\theta)\frac{\overline{z}^2}{2}+\cdots .$$

Then the flow of system (4.2) on the central manifold C_0 is determined by the equation

$$\dot{z}(t)=i\hat{\omega}\hat{\tau}\,\langle q^*(s), X_t\rangle+\overline{q^*}(0)f(0,X_t(\theta)) =: i\hat{\omega}\hat{\tau}z(t)+\overline{q^*}(0)G_0,$$

where $G_0=G(0,z(t)q(\theta)+\overline{z}(t)\overline{q}(\theta)+W(z,\overline{z},\theta))$. Denote

$$\begin{aligned}
&G_0=G_{z^2}\frac{z^2}{2}+G_{z\bar{z}}z\overline{z}+G_{\bar{z}^2}\frac{\overline{z}^2}{2}+G_{z^2\bar{z}}\frac{z^2\overline{z}}{2}+\cdots,\\
&g(z,\bar{z})=\overline{q^*}(0)G_0=\overline{D}(1,\overline{\gamma^*})\begin{pmatrix} G_1(0,X_t)\\ G_2(0,X_t)\end{pmatrix}=\overline{D}(G_1(0,X_t)+\overline{\gamma^*}G_2(0,X_t)),
\end{aligned}$$

and $z(t)$ satisfies

$$\dot{z}(t)=i\hat{\omega}\hat{\tau}z(t)+g(z,\bar{z})(t). \tag{4.3}$$

Let

$$g(z,\bar{z})=g_{20}\frac{z^2}{2}+g_{11}z\overline{z}+g_{02}\frac{\overline{z}^2}{2}+g_{21}\frac{z^2\overline{z}}{2}+\cdots .$$

The coefficients g_{20}, g_{11}, g_{02}, and g_{21} can be calculated as follows:

$$\begin{aligned}
g_{20}&=2\overline{D}\hat{\tau}\left[\gamma e^{-2i\hat{\omega}\hat{\tau}}(m_1+m_2\gamma)+n_1-a+n_2\gamma-c\overline{\gamma^*}(n_1+n_2\gamma)\right],\\
g_{11}&=\overline{D}\hat{\tau}\left[m_1(\gamma+\overline{\gamma})+2m_2\gamma\overline{\gamma}+2(n_1-a)+n_2(\gamma+\overline{\gamma})-c\overline{\gamma^*}(2n_1+n_2(\gamma+\overline{\gamma}))\right],\\
g_{02}&=2\overline{D}\hat{\tau}\left[\overline{\gamma}e^{2i\hat{\omega}\hat{\tau}}(m_1+m_2\overline{\gamma})+n_1-a+n_2\overline{\gamma}-c\overline{\gamma^*}(n_1+n_2\overline{\gamma})\right],\\
g_{21}&=2\overline{D}\hat{\tau}\Bigg\{m_1\left(e^{-i\hat{\omega}\hat{\tau}}W_{11}^{(2)}(-1)+\frac{e^{i\hat{\omega}\hat{\tau}}}{2}W_{20}^{(2)}(-1)+\frac{e^{i\hat{\omega}\hat{\tau}}}{2}\overline{\gamma}W_{20}^{(1)}(-1)+\gamma e^{-i\hat{\omega}\hat{\tau}}W_{11}^{(1)}(-1)\right)\\
&\quad+m_2\left(2\gamma e^{-i\hat{\omega}\hat{\tau}}W_{11}^{(2)}(-1)+\overline{\gamma}e^{i\hat{\omega}\hat{\tau}}W_{20}^{(2)}(-1)\right)+m_3\gamma e^{-i\hat{\omega}\hat{\tau}}(\gamma+2\overline{\gamma})+3m_4\gamma^2\overline{\gamma}e^{-i\hat{\omega}\hat{\tau}}\\
&\quad+(n_1-a)\left(W_{20}^{(1)}(0)+2W_{11}^{(1)}(0)\right)+n_2\left(\gamma W_{11}^{(1)}(0)+\frac{\overline{\gamma}}{2}W_{20}^{(1)}(0)+\frac{1}{2}W_{20}^{(2)}(0)+W_{11}^{(2)}(0)\right)\\
&\quad+3n_3+n_4(\overline{\gamma}+2\gamma)-c\overline{\gamma^*}\Bigg[n_1\left(W_{20}^{(1)}(0)+2W_{11}^{(1)}(0)\right)+n_2\Bigg(\gamma W_{11}^{(1)}(0)+\frac{\overline{\gamma}}{2}W_{20}^{(1)}(0)\\
&\quad+\frac{1}{2}W_{20}^{(2)}(0)+W_{11}^{(2)}(0)\Bigg)+3n_3+n_4(\overline{\gamma}+2\gamma)\Bigg]\Bigg\},
\end{aligned}$$

where

$$\begin{aligned}
W_{20}(\theta)&=\frac{ig_{20}}{\hat{\omega}\hat{\tau}}q(0)e^{i\hat{\omega}\hat{\tau}\theta}+\frac{i\overline{g}_{02}}{3\hat{\omega}\hat{\tau}}\overline{q}(0)e^{-i\hat{\omega}\hat{\tau}\theta}+E_1e^{2i\hat{\omega}\hat{\tau}\theta},\\
W_{11}(\theta)&=-\frac{ig_{11}}{\hat{\omega}\hat{\tau}}q(0)e^{i\hat{\omega}\hat{\tau}\theta}+\frac{i\overline{g}_{11}}{\hat{\omega}\hat{\tau}}\overline{q}(0)e^{-i\hat{\omega}\hat{\tau}\theta}+E_2,
\end{aligned}$$

and $E_1 = (E_1^{(1)}, E_1^{(2)})^T \in \mathbb{R}^2$, $E_2 = (E_2^{(1)}, E_2^{(2)})^T \in \mathbb{R}^2$ satisfy

$$E_1 = 2\begin{pmatrix} 2i\hat{\omega} - b_1 - c_1 e^{-2i\hat{\omega}\hat{\tau}} & -b_2 - c_2 e^{-2i\hat{\omega}\hat{\tau}} \\ -b_3 & 2i\hat{\omega} \end{pmatrix}^{-1} \begin{pmatrix} \gamma e^{-2i\hat{\omega}\hat{\tau}}(m_1 + m_2\gamma) + n_1 - a + n_2\gamma \\ -c(n_1 + n_2\gamma) \end{pmatrix},$$

$$E_2 = -\begin{pmatrix} b_1 + c_1 & b_2 + c_2 \\ b_3 & 0 \end{pmatrix}^{-1} \begin{pmatrix} (m_1 + n_2)(\gamma + \overline{\gamma}) + 2m_2\gamma\overline{\gamma} + 2(n_1 - a) \\ -c[2n_1 + n_2(\gamma + \overline{\gamma})] \end{pmatrix}.$$

Consequently, we obtain

$$\begin{aligned} c_1(0) &= \frac{i}{2\hat{\omega}\hat{\tau}}\left(g_{11}g_{20} - 2\left|g_{11}\right|^2 - \frac{\left|g_{02}\right|^2}{3}\right) + \frac{g_{21}}{2}, \\ \mu_2 &= -\frac{\mathrm{Re}(c_1(0))}{\mathrm{Re}(\lambda'(\hat{\tau}))}, \quad \beta_2 = 2\mathrm{Re}(c_1(0)). \end{aligned} \tag{4.4}$$

By the theory of normal forms and central manifold for delay (or functional) differential equations in [17], the above expressions determines the direction and stability of the Hopf bifurcation at $\tau = \hat{\tau}$ as stated in the following theorem.

THEOREM 4.1. *The following statements hold:*

(i) *If $\mu_2 > 0$ ($\mu_2 < 0$), the bifurcated periodic solution appears for τ in the right neighborhood (left neighborhood) of $\hat{\tau}$.*

(ii) *If $\beta_2 < 0$ ($\beta_2 > 0$), the bifurcated periodic solution is asymptotically orbital stable (unstable).*

5. Numerical simulations.

In this section, we present some numerical simulations to illustrate the main analytic results obtained in the preceding sections. These simulations can more visually demonstrate the impact of the prey's maturation delay. For this purpose, we will refer to some sets of parameter values in [37] under three different scenarios, as this will make comparison convenient/straightforward.

5.1. Case of two periodic solutions when $\tau = 0$.

We choose the following parameter set and fixed $k = 60$, which is consistent with the parameters of Figure 7 in [37]:

$$r_0 = 0.12,\ d = 0.01,\ a = 0.01,\ p = 0.5,\ q = 0.6,\ c = 0.4,\ m = 0.05,\ d_0 = 0.1. \tag{5.1}$$

With (5.1), model (3.6) has a subcritical Hopf bifurcation occurring at $k = k^* = 58.2352$ (see Lemma 3.6). From (3.4) and (3.5), we obtain $\tau_* \approx 24.8491$, $\tau_{**} \approx 22.2708$. By Theorem 3.5, if $\tau \in [24.8491, +\infty)$, the trivial equilibrium E_0 is globally asymptotically stable; if $\tau \in [22.2708, 24.8491)$, the boundary equilibrium E_1 is globally asymptotically stable; if $\tau \in [0, 22.2708)$, there exists a unique positive equilibrium E^*.

For the set of parameters given in (5.1), the numerical simulation result in Wang, Zanette, and Zou [37] shows that system (3.6) has a stable positive equilibrium E^*, a stable periodic solution, and an unstable periodic solution that bifurcates near E^*. That is, the corresponding ODE model exhibits a bistability phenomenon: if the initial value is within the unstable limit cycle, prey and predators will tend to a steady state, and if the initial value is larger, outside the unstable limit cycle, the populations of prey and predator oscillate periodically. Now let us look at the situation when the maturation delay τ is incorporated. Figure 1(a) gives the graph of $S_0(\tau)$ and $S_1(\tau)$ defined by (3.15) for $\tau \in [0, \tau_{**})$. As can be seen from Figure 1(a), $S_n(\tau) = 0$ does not have positive roots for any $n \geqslant 1$, and $S_0(\tau)$ has two zeros, denoted by τ_1, τ_2, where

$$\tau_1 \approx 0.0614,\ \tau_2 \approx 17.2473.$$

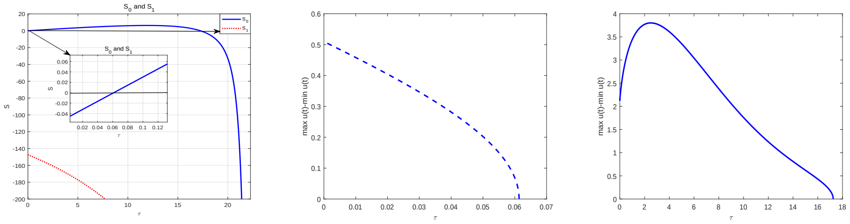

(a) $S_0(\tau),\ S_1(\tau),\ \tau \in [0, \tau_{**})$ (b) Bifurcation diagram at τ_1 (c) Bifurcation diagram at τ_2

FIG. 1. *Bifurcation points and bifurcation diagram for model* (1.4) *with* $k = 60$ *and other parameters given in* (5.1).

By (3.16), there hold $S_0'(\tau_1) > 0$ and $S_0'(\tau_2) < 0$. Thus, Hopf bifurcation occurs at τ_1 and τ_2 by Theorem 3.9. Direct calculations give that when $\tau = \tau_1$, $\mathrm{Re}(c_1(0)) \approx 0.0001 > 0$; when $\tau = \tau_2$, $\mathrm{Re}(c_1(0)) \approx -0.3491 < 0$. Then $\mu_2(\tau_1) < 0$, $\mu_2(\tau_2) < 0$. Consequently, according to Theorem 4.1, the bifurcated periodic solution bifurcating from τ_1 is unstable and appears in the *left neighborhood of* τ_1; the bifurcated periodic solution bifurcating from τ_2 is stable and appears in the *left neighborhood of* τ_2. Moreover, if $\tau \in [0, \tau_1) \cup (\tau_2, \tau_{**})$, all characteristic roots of (3.12) have strictly negative real parts and E^* is locally asymptotically stable; if $\tau \in (\tau_1, \tau_2)$, there exists a pair of characteristic roots with strictly positive real parts and E^* is unstable.

With the help of the DDE-BIFTOOL package in [13], we plot the diagram of global Hopf bifurcation with respect to delay τ in Figure 1. In (b) and (c) of Figure 1, the horizontal coordinate represents delay τ, and the vertical coordinate represents the amplitude of the periodic solution. Each point on the dashed curve in (b) represents an unstable periodic solution, and each point on the solid curve in (c) represents a stable periodic solution. We found that the local unstable Hopf bifurcation bifurcating from τ_1 exists globally at the left side of τ_1 until $\tau = 0$. The locally stable Hopf bifurcation bifurcating from τ_2 also exists globally at the left side of τ_2 until $\tau = 0$, implying that the bistable scenario observed in [37] for (3.6) (i.e., $\tau = 0$ in (1.4)) actually remains valid for (1.4) when $\tau \in (0, \tau_1)$.

Next, we performed simulations near τ_1 and τ_2 to illustrate the stability of E^*. Choosing $\tau = 0.02 < \tau_1$, the positive equilibrium E^* is $(u^*, v^*) = (0.2941, 0.0454)$. Note that (b) and (c) of Figure 1 show that there exist an unstable periodic solution and a stable periodic solution. Figure 2(a) indicates that our model inhibits the bistability phenomenon: the populations of prey and predator tend to a locally stable periodic solution if the initial values are outside the unstable limit cycle, and when the initial value is smaller, within the unstable limit cycle, populations will approach a positive steady state. Therefore, the bistability phenomenon generated by system (3.6) will not disappear when the introduced delay τ is small ($\tau \in (0, \tau_1) = (0, 0.0614)$), as shown in Figure 2(a). If $\tau_1 < \tau < \tau_2$, E^* loses its stability, and Figure 1(c) shows that there exists a stable periodic solution meaning that all the solution will converge to the stable periodic solution (as demonstrated in Figure 2(b) for $\tau = 0.1 \in (\tau_1, \tau_2)$ and Figure 2(c) for $\tau = 16.5 \in (\tau_1, \tau_2)$.

Near τ_2, the simulations show that with the increase of delay passing τ_2, the stable periodic solution disappears, merging with and yielding its stability to the coexistence equilibrium E^*, making E^* globally asymptotically stable. See Figures 2(c) and 2(d) for a demonstration.

5.2. Case of one periodic solution when $\tau = 0$.

Fix $k = 40$ and let other parameters remain the same as in (5.1). For model (3.6), the positive equilibrium is

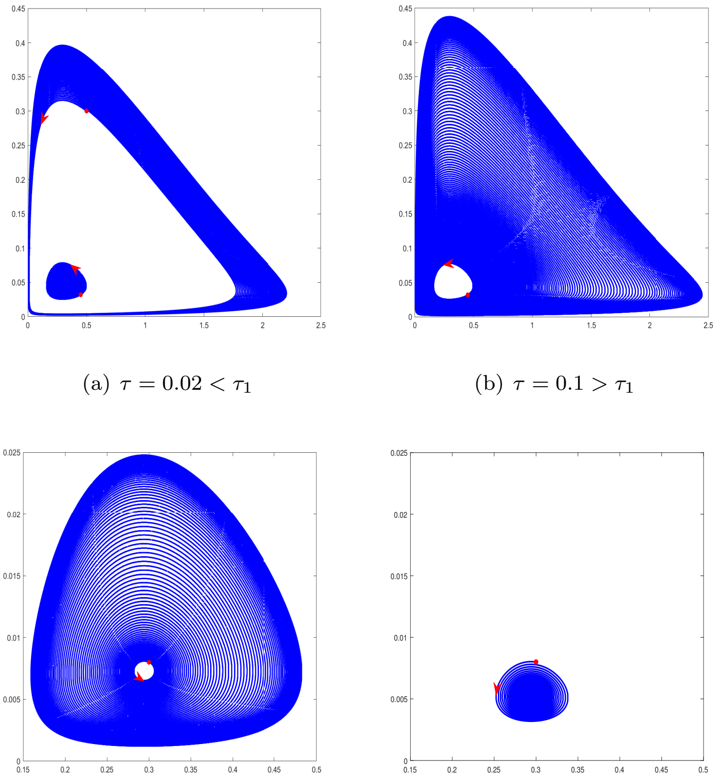

(a) $\tau = 0.02 < \tau_1$

(b) $\tau = 0.1 > \tau_1$

(c) $\tau = 16.5 < \tau_2$

(d) $\tau = 18 > \tau_2$

FIG. 2. *Dynamical behaviors of model* (1.4) *with* $k = 60$ *and other parameters given in* (5.1). *Here the red star represents the initial value, and the red arrow indicates the direction of the trajectory. (Color available online.)*

unstable and there exists a stable periodic solution. As τ_* and τ_{**} are independent of k, we just need to see the dynamics of model (1.4) when $\tau \in [0, \tau_{**})$.

The simulations tell us that there exists a unique $\tau_c \approx 2.5903$ which is a first type of discontinuity point of $S_n(\tau)$ and it is not a root of the characteristic equation (3.12). Figure 3(a) depicts the graphs of $S_0(\tau)$ and $S_1(\tau)$, while Figure 3(b) is just a vertical rescaling of Figure 3(a) to the range of $[-1, 7]$ for $\tau \in (\tau_c, \tau_{**}) = (2.5903, 22.2708)$. We found that there exists

$$\tau_3 \approx 16.8381$$

such that $S_0(\tau_3) = 0$ with $\delta(\tau_3) = S_0'(\tau_3) < 0$ and $S_n(\tau)$ has no zeros for any $n \geqslant 1$. By Theorem 3.10, Hopf bifurcation occurs at $\tau = \tau_3$. Moreover, we calculate that when $\tau = \tau_3$, $\mathrm{Re}(c_1(0)) \approx -0.1729 < 0$. Then $\mu_2(\tau_3) < 0$, implying that the bifurcated periodic solution bifurcating from τ_3 is stable and appears in the *left neighborhood of* τ_3. We also plot the global Hopf bifurcation diagram in Figure 3(c), which shows that if $0 < \tau < \tau_3$, populations of predator and prey tend to the stable bifurcated periodic solution. The population dynamics of (1.4) in this situation are similar to that for the model (3.6). When $\tau_3 < \tau < \tau_{**}$, the periodic solution disappears, merging with the coexistence equilibrium E^*, which becomes stable.

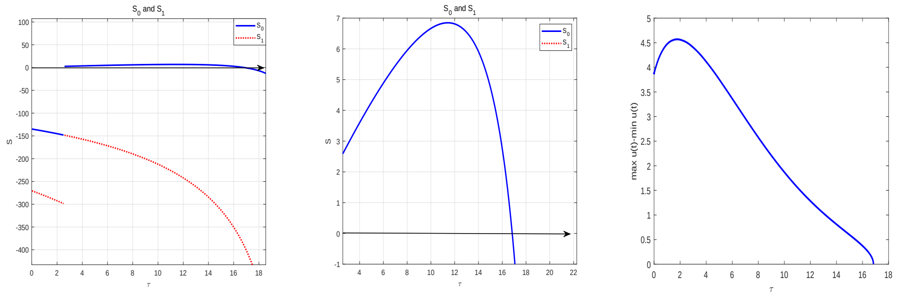

(a) $S_0(\tau)$ and $S_1(\tau)$

(b) The local graph of $S_0(\tau)$ and $S_1(\tau)$

(c) Global Hopf bifurcation diagram

FIG. 3. *Bifurcation points and bifurcation diagram for model* (1.4) *with* $k = 40$ *and other parameters given in* (5.1).

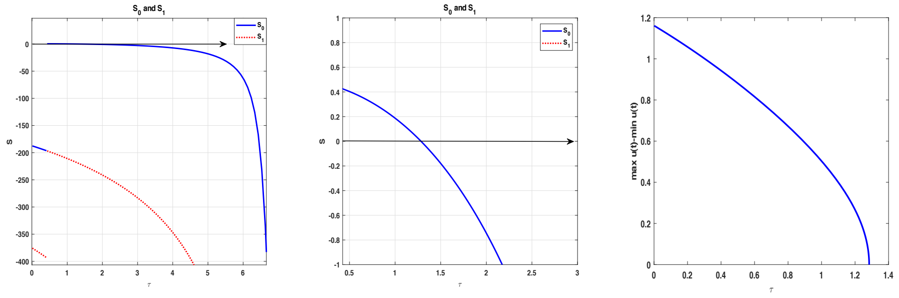

(a) $S_0(\tau)$ and $S_1(\tau)$

(b) The local graph of $S_0(\tau)$, $S_1(\tau)$

(c) Global Hopf bifurcation diagram

FIG. 4. *Bifurcation points and bifurcation diagram for model* (1.4) *with* $k = 30$ *and other parameters given in* (5.2).

Fix $k = 30$ and the other parameters as shown in (5.2) below. For this set of parameters, model (3.6) has a supercritical Hopf bifurcation occurring at $k = k^* = 35.1563$ by Lemma 3.6. The positive equilibrium is unstable because of $k = 30 < k^*$, and there exists a stable periodic solution.

$$r_0 = 0.06,\ d = 0.01,\ a = 0.01,\ p = 0.5,\ q = 1,\ c = 0.4,\ m = 0.05,\ d_0 = 0.2. \tag{5.2}$$

For this set of parameters, (3.4) and (3.5) are calculated as $\tau_* = 8.9588$, $\tau_{**} = 7.5204$. By Theorem 3.5, if $\tau \in [8.9588, +\infty)$, E_0 is globally asymptotically stable; if $\tau \in [7.5204, 8.9588)$, E_1 is globally asymptotically stable.

Within $(0, 7.5204)$, there exists a unique $\tau_c \approx 0.4251$ which is the first type discontinuity point of $S_n(\tau)$, and it is not the root of the characteristic equation (3.12). Figure 4(a) gives the graph of $S_0(\tau)$ and $S_1(\tau)$, and Figure 4(b) is the local graph of $S_0(\tau)$ and $S_1(\tau)$ for $\tau \in (0.4251, 7.5204)$. We found that $S_n(\tau)$ does not have zeros for all $n \geqslant 1$ and $S_0(\tau)$ has a unique zero, $\tau_4 \approx 1.2841$ with $\delta(\tau_4) = S_0'(\tau_4) < 0$. Thus, Hopf bifurcation occurs at $\tau = \tau_4$ by Theorem 3.10. Further, we have $\mathrm{Re}(c_1(0)) \approx -0.0034 < 0$ when $\tau = \tau_4$, and hence $\mu_2(\tau_4) < 0$, meaning that the bifurcated periodic solution appears in the *left neighborhood of* τ_4 and is stable (see Figure 4(c)).

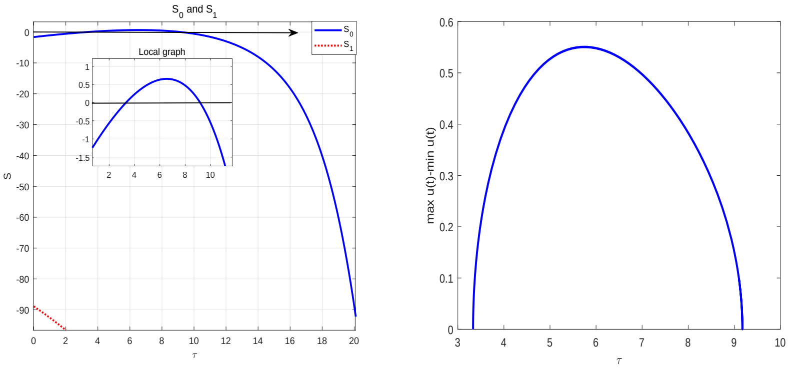

(a) $S_0(\tau)$ and $S_1(\tau)$ (b) Global Hopf bifurcation diagram

FIG. 5. *Bifurcation points and bifurcation diagram for model* (1.4) *with* $k = 20$ *and other parameters given in* (5.3).

5.3. Case of no periodic solution when $\tau = 0$. With the parameters given by

$$r_0 = 0.4,\ d = 0.01,\ a = 0.05,\ p = 0.5,\ q = 0.6,\ c = 0.4,\ m = 0.05,\ d_0 = 0.1, \tag{5.3}$$

ODE model (3.6) has a supercritical Hopf bifurcation occurring at $k = k^* = 9.7918$. Take $k = 20 > k^*$ so that the positive equilibrium E^* is locally asymptotically stable. Then we can numerically calculate the critical values in (3.4) and (3.5) as $\tau_* = 36.8888$, $\tau_{**} = 27.8442$. By Theorem 3.5, if $\tau \geq 36.8888$, E_0 is globally asymptotically stable; if $\tau \in [27.8442,\ 36.8888)$, E_1 is globally asymptotically stable. Moreover, for $0 < \tau < 27.8442$, Figure 5(a) shows that $S_n(\tau) = 0$ does not have positive real root for all $n \geqslant 1$ and $S_0(\tau) = 0$ has two positive real roots

$$\tau_5 \approx 3.3311,\ \tau_6 \approx 9.1766,$$

at which $\delta(\tau_5) = S_0'(\tau_5) > 0$ and $\delta(\tau_6) = S_0'(\tau_6) < 0$. By Theorem 3.9, Hopf bifurcation occurs at τ_5 and τ_6. Furthermore, $\mathrm{Re}(c_1(0)) \approx -0.0378 < 0$ when $\tau = \tau_5$ and $\mathrm{Re}(c_1(0)) \approx -0.1012 < 0$ when $\tau = \tau_6$, implying that $\mu_2(\tau_5) > 0$ and $\mu_2(\tau_6) < 0$. Therefore, the bifurcated periodic solution bifurcating from τ_5 is stable and appears in the *right neighborhood of* τ_5; the bifurcated periodic solution bifurcating from τ_6 is stable and appears in the *left neighborhood of* τ_6. The global Hopf bifurcation diagram is presented in Figure 5(b), which shows that the two bifurcated periodic solutions actually merge for $\tau \in (\tau_5, \tau_6) = (36.8888, 27.8442)$. In this case, with the increase of delay, the periodic solution appears (E^* loses its stability) and then disappears (E^* regains its stability).

If the parameter values in (5.3) are replaced by

$$r_0 = 0.03,\ d = 0.01,\ a = 0.01,\ p = 0.5,\ q = 0.1,\ c = 0.4,\ m = 0.05,\ d_0 = 0.1, \tag{5.4}$$

then straightforward calculations show that condition (3.7) holds and there is no Hopf bifurcation for ODE model (3.6) for any $k > 0$ because of $k^* = -3.5146 < 0$. Thus, the positive equilibrium of model (3.6) is always locally asymptotically stable for any $k > 0$. In the meantime, two critical values in (3.4) and (3.5) are now calculated to be $\tau_* = 10.9861$, $\tau_{**} = 8.7035$. By Theorem 3.5, if $\tau \geq 10.9861$, E_0 is globally asymptotically stable; if $\tau \in [8.7035,\ 10.9861)$, E_1 is globally asymptotically stable; and if $\tau \in [0, 8.7035)$, system (1.4) has a unique positive equilibrium E^*. With the help of MATLAB, there is no Hopf bifurcation. Hence, for any $\tau \in [0, 8.7035)$, E^* is globally asymptotically stable. We conclude that with the parameter set (5.4), the delay τ will not impact the stability of E^*, meaning that as long as it exists, it is globally asymptotically stable.

6. Summary and conclusion.

In this paper, we have modified the existing ODE predator-prey model with the fear effect as defined in [37] by incorporating the maturation delay, leading to a delay differential equation (DDE) system for the interaction of the predator and prey. This modification turns a finite-dimensional dynamical system to an infinite-dimensional system (1.4). We have addressed the well-posedness of the new model system and thoroughly analyzed its dynamics. We have found that the new DDE system has rich dynamics, meaning that within different ranges of the model parameters, including the maturation delay as a new parameter in comparison with the ODE model in [37], there can be various asymptotical behaviors. Particularly, we have explored the impact of the maturation delay τ within various scenarios for the corresponding ODE model (3.6).

Our mathematical results show that for the new DDE model, there exist two critical values, denoted τ_* and τ_{**}. If $0 < \tau < \tau_{**}$, the prey and predator populations will co-persist, tending either to a stable positive equilibrium or to a stable periodic solution. This suggests that smaller time delay is beneficial to the survival of both prey and predator populations. If $\tau_{**} < \tau < \tau^*$, however, the predator will go extinct and the prey will tend to a positive steady state. This is because if the maturation period is long but not too long, the rate of the immature prey entering the mature stage would be small but not too small, leading to a lack of adult prey for the predator to predate. Such a lack may then drive the predator to extinction since we have assumed that the predator is a specialist predator and it only predates on the matured prey. If the maturation period is too long, the prey itself cannot survive, let alone the specialist predator, a scenario implied by the global asymptotical stability of the extinction equilibrium E_0.

Most interesting is the dynamics of DDE model (1.4) when the delay τ is in the *intermediate range,* which is a reality for many prey species. In this range, we have seen that, depending on other parameters, there can be different long-term dynamics corresponding to the bifurcations about the positive equilibrium E^* caused by the delay τ, as presented in Theorems 3.9 and 3.10.

Some numerical simulations further reveal that the bifurcations obtained in Theorems 3.9 and 3.10 are actually global. The respective bifurcation diagrams depict, within different ranges of the fear effect level k, how the time delay can affect the stability, causing stability switches (some are cascaded switches). For the reader's convenience, we organize the bifurcation diagrams in Figure 6 for (3.6) and (1.4) with the respective given parameter sets. An interesting result observed from Figure 6 is that the stability of the positive equilibrium in model (1.4) changes from stable to unstable to stable as τ increases (see the cases of (5.1) with $k = 60$ and (5.3) with $k = 20$ in Figure 6). At the same time, Hopf bifurcation occurred when the stability changes, meaning that the unstable and stable periodic solutions in ODE model (3.6) disappear successively as the maturation delay increases, as shown in the case of (5.1) with $k = 60$ of Figure 6. Another interesting result is that the stability of positive equilibrium changes from unstable to stable, and the stable periodic solution in ODE model (3.6) disappears when stability reversal happens (see the case of (5.1) with $k = 40$ and (5.2) with $k = 30$ in Figure 6).

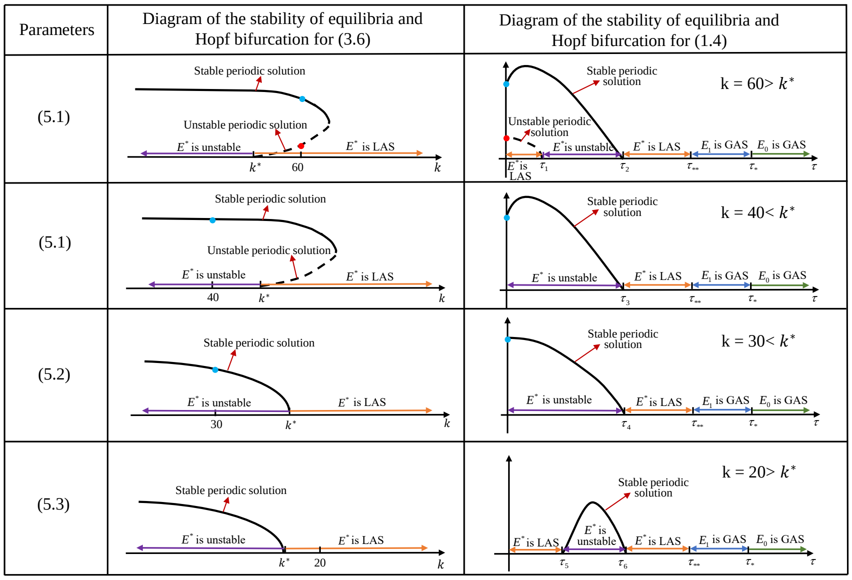

FIG. 6. *Dynamics of model* (1.4) *when subcritical or supercritical Hopf bifurcation occurs for ODE model* (3.6) *where the y-coordinate represents the amplitude of the periodic solution.*

In conclusion, both stable and unstable periodic solutions in the corresponding ODE model [37] may disappear as time delay increases. Moreover, as given in the case of (5.3) with $k = 20$, when the positive equilibrium is locally asymptotically stable in ODE model (3.6), a periodic solution appears and then disappears as the delay increases. Our results reveal how the maturation delay and the fear effect jointly impact the population dynamics of the predator-prey system and suggest certain parameter ranges for coexistence of both the predator and prey, which is a desired goal for the purpose of biodiversity.

Acknowledgments. We would like to thank Dr. Chuncheng Wang for his help on numerical simulations. We are very grateful to the three anonymous referees for their valuable comments which have led to an improvement in the presentation of the paper.

REFERENCES

[1] K. B. Altendorf, J. W. Laundré, C. A. López González, and J. S. Brown, *Assessing effects of predation risk on foraging behavior of mule deer*, J. Mammal., 82 (2001), pp. 430–439.

[2] R. Banerjee, P. Das, and D. Mukherjee, *Effects of fear and anti-predator response in a discrete system with delay*, Discrete Contin. Dyn. Syst. Ser. B, 27 (2022), pp. 3643–3661.

[3] D. Barman, J. Roy, and S. Alam, *Trade-off between fear level induced by predator and infection rate among prey species*, J. Appl. Math. Comput., 64 (2020), pp. 635–663.

[4] J. R. Beddington, *Mutual interference between parasites or predators and its effect on searching efficiency*, J. Animal Ecol., (1975), pp. 331–340.

[5] E. Beretta and Y. Kuang, *Geometric stability switch criteria in delay differential systems with delay dependent parameters*, SIAM J. Math. Anal., 33 (2002), pp. 1144–1165, https://doi.org/10.1137/S0036141000376086.

[6] S. Creel and D. Christianson, *Relationships between direct predation and risk effects*, Trends Ecol. Evol., 23 (2008), pp. 194–201.

[7] W. Cresswell, *Predation in bird populations*, J. Ornithol., 152 (2011), pp. 251–263.

[8] B. Dai and G. Sun, *Turing–Hopf bifurcation of a delayed diffusive predator–prey system with chemotaxis and fear effect*, Appl. Math. Lett., 111 (2021), 106644.

[9] A. Das and G. Samanta, *Modeling the fear effect on a stochastic prey–predator system with additional food for the predator*, J. Phys. A, 51 (2018), 465601.

[10] D. L. DeAngelis, R. Goldstein, and R. V. O'Neill, *A model for tropic interaction*, Ecology, 56 (1975), pp. 881–892.

[11] D. Duan, B. Niu, and J. Wei, *Hopf-Hopf bifurcation and chaotic attractors in a delayed diffusive predator-prey model with fear effect*, Chaos Solitons Fractals, 123 (2019), pp. 206–216.

[12] B. Dubey, Sanjan, and A. Kumar, *Stability switching and chaos in a multiple delayed prey–predator model with fear effect and anti-predator behavior*, Math. Comput. Simul., 188 (2021), pp. 164–192.

[13] K. Engelborghs, T. Luzyanina, and G. Samaey, *DDE-BIFTOOL v.* 2.00*: A MATLAB Package for Bifurcation Analysis of Delay Differential Equations*, Report TW305, K.U. Leuven, 2000.

[14] C. K. Ghalambor, S. I. Peluc, and T. E. Martin, *Plasticity of parental care under the risk of predation: How much should parents reduce care?*, Biol. Lett., 9 (2013), 20130154.

[15] S. Halder, J. Bhattacharyya, and S. Pal, *Comparative studies on a predator–prey model subjected to fear and Allee effect with type* I *and type* II *foraging*, J. Appl. Math. Comput., 62 (2020), pp. 93–118.

[16] J. K. Hale, *Theory of Functional Differential Equations*, Springer, 1977.

[17] B. D. Hassard, N. D. Kazarinoff, and Y.-H. Wan, *Theory and Applications of Hopf Bifurcation*, London Math. Soc. Lecture Note Ser. 41, Cambridge University Press, 1981.

[18] C. S. Holling, *The functional response of predators to prey density and its role in mimicry and population regulation*, Mem. Entomol. Soc. Canada, 97 (1965), pp. 5–60.

[19] A. Kumar and B. Dubey, *Modeling the effect of fear in a prey–predator system with prey refuge and gestation delay*, Internat. J. Bifur. Chaos, 29 (2019), 1950195.

[20] L. Lai, X. Yu, M. He, and Z. Li, *Impact of Michaelis–Menten type harvesting in a Lotka–Volterra predator–prey system incorporating fear effect*, Adv. Difference Equations, 2020 (2020), pp. 1–22.

[21] A. Li and X. Zou, *Evolution and adaptation of anti-predation response of prey in a two-patchy environment*, Bull. Math. Biol., 83 (2021), pp. 1–27.

[22] T. Li and Q. Wang, *Turing patterns in a predator–prey reaction–diffusion model with seasonality and fear effect*, J. Nonlinear Sci., 33 (2023), 86.

[23] A. J. Lotka, *Elements of Physical Biology*, Williams & Wilkins, Philadelphia, 1925.

[24] S. Pal, N. Pal, S. Samanta, and J. Chattopadhyay, *Fear effect in prey and hunting cooperation among predators in a Leslie-Gower model*, Math. Biosci. Eng., 16, pp. 5146–5179.

[25] P. Panday, N. Pal, S. Samanta, and J. Chattopadhyay, *Stability and bifurcation analysis of a three-species food chain model with fear*, Internat. J. Bifur. Chaos, 28 (2018), 1850009.

[26] P. Panday, S. Samanta, N. Pal, and J. Chattopadhyay, *Delay induced multiple stability switch and chaos in a predator–prey model with fear effect*, Math. Comput. Simul., 172 (2020), pp. 134–158.

[27] J. Roy and S. Alam, *Fear factor in a prey–predator system in deterministic and stochastic environment*, Phys. A, 541 (2020), 123359.

[28] S. Ruan and J. Wei, *On the zeros of transcendental functions with applications to stability of delay differential equations with two delays*, Dyn. Contin. Discrete Impuls. Syst. Ser. A, 10 (2003), pp. 863–874.

[29] S. Ruan and D. Xiao, *Global analysis in a predator-prey system with nonmonotonic functional response*, SIAM J. Appl. Math., 61 (2001), pp. 1445–1472, https://doi.org/10.1137/S0036139999361896.

[30] H. Smith, *An Introduction to Delay Differential Equations with Applications to the Life Sciences*, Springer, 2011.

[31] H. Smith and X. Q. Zhao, *Robust persistence for semidynamical systems*, Nonlinear Anal., 47 (2001), pp. 6169–6179.

[32] H. L. Smith, *Monotone Dynamical Systems: An Introduction to the Theory of Competitive and Cooperative Systems*, Math. Surveys Monogr. 41, American Mathematical Society, 1995.

[33] Y. Song and X. Zou, *Bifurcation analysis of a diffusive ratio-dependent predator–prey model*, Nonlinear Dyn., 78 (2014), pp. 49–70.

[34] H. R. Thieme, *Convergence results and a Poincaré-Bendixson trichotomy for asymptotically autonomous differential equations*, J. Math. Biol., 30 (1992), pp. 755–763.

[35] R. K. Upadhyay and S. Mishra, *Population dynamic consequences of fearful prey in a spatiotemporal predator-prey system*, Math. Biosci. Eng., 16 (2018), pp. 338–372.

[36] V. Volterra, *Variazioni e fluttuazioni del numero d'individui in specie animali conviventi*, Societá anonima tipografica "Leonardo da Vinci," 2 (1927).

[37] X. Wang, L. Zanette, and X. Zou, *Modelling the fear effect in predator–prey interactions*, J. Math. Biol., 73 (2016), pp. 1179–1204.

[38] X. Wang and X. Zou, *Modeling the fear effect in predator–prey interactions with adaptive avoidance of predators*, Bull. Math. Biol., 79 (2017), pp. 1325–1359.

[39] X. Wang and X. Zou, *Pattern formation of a predator-prey model with the cost of anti-predator behaviors*, Math. Biosci. Eng., 15 (2017), pp. 775–805.

[40] Y. Wang and X. Zou, *On a predator–prey system with digestion delay and anti-predation strategy*, J. Nonlinear Sci., 30 (2020), pp. 1579–1605.

[41] L. Y. Zanette, A. F. White, M. C. Allen, and M. Clinchy, *Perceived predation risk reduces the number of offspring songbirds produce per year*, Science, 334 (2011), pp. 1398–1401.

[42] H. Zhang, Y. Cai, S. Fu, and W. Wang, *Impact of the fear effect in a prey-predator model incorporating a prey refuge*, Appl. Math. Comput., 356 (2019), pp. 328–337.